Supplementary Materials for

Gasdermin D drives focal Crystalline Thrombotic Microangiopathy by accelerating Immunothrombosis and Necroinflammation

Kanako Watanabe-Kusunoki[1,2], Chenyu Li[1], Tâmisa Seeko Bandeira Honda[1], Danyang Zhao[1], Yoshihiro Kusunoki[1,2], John Ku[1], Hao Long[1,3], Martin Klaus[1], Chao Han[1,4], Attila Braun[1,4], Elmina Mammadova-Bach[1,4], Andreas Linkermann[5,6], Kristof Van Avondt[7], Mathis Richter[7], Oliver Soehnlein[7], Monika I. Linder[8], Christoph Klein[8], Stefanie Steiger[1,#], Hans-Joachim Anders[1,#]

1 Renal Division, Department of Medicine IV, LMU University Hospital, LMU Munich, Germany
2 Department of Rheumatology, Endocrinology and Nephrology, Faculty of Medicine and Graduate School of Medicine, Hokkaido University, Sapporo, Japan
3 Department of Urology, The Affiliated Hospital of Southwest Medical University, Luzhou, China
4 Walther-Straub-Institute for Pharmacology and Toxicology, Ludwig-Maximilians-University, Munich, Germany
5 Department of Internal Medicine 3, University Hospital Carl Gustav Carus at the Technische Universität Dresden, Dresden, Germany
6 Division of Nephrology, Department of Medicine, Albert Einstein College of Medicine, Bronx, New York, United States
7 Institute of Experimental Pathology (ExPat), Centre of Molecular Biology of Inflammation (ZMBE), University of Münster, Münster, Germany
8 Department of Pediatrics, Dr. von Hauner Children's Hospital, University Hospital, Ludwig-Maximilians-Universität (LMU), Munich, Germany
# contributed equally.

This file includes:

Supplementary Methods

Cholesterol crystal preparation

The preparation of cholesterol crystal (CC) was performed as previously described. Briefly, for animal studies, 25 mg cholesterol (Sigma-Aldrich, Steinheim, Germany) was suspended in 5 mL sterile phosphate-buffered saline (PBS), sonicated, and filtered through a 33-gauge needle immediately prior to use.[1] For in vitro studies, cholesterol was solubilized in 95% ethanol at a concentration of 12.5 mg/mL by heating to 65°C. Crystallization was induced by subsequent cooling on ice. After five cycles of recrystallization, the crystals were collected and suspended in PBS at a concentration of 5 mg/mL.[2]

Induction of focal crystalline thrombotic microangiopathy (TMA)

Six- to eight-week-old male mice were anaesthetized via intraperitoneal injection of medetomidine (0.5 mg/kg), midazolam (5 mg/kg), and fentanyl (0.05 mg/kg) and maintained in a heat chamber for body temperature control. During surgical procedures, body temperature was sustained by placing the mice on a heating pad. CC (20 mg/kg) was administered into the left renal artery via a 33-gauge needle, and the injection was verified through the alteration of color in the left kidney from red to white. Following bleeding control and wound closure, the mice received antagonists (atipamezole 2.5 mg/kg and flumazenil 0.5 mg/kg) and pain management with buprenorphine (0.1 mg/kg). Immediately after measurement of glomerular filtration rate (GFR) at 24 hours post-surgery, the mice were sacrificed for analysis. Insufficient decolorization of the left kidney after injection or an increase in GFR at 24 hours post-surgery were considered as technical failures and excluded from the analysis. The right (contralateral healthy) kidneys were used as an internal sham control.

Disulfiram treatment in focal crystalline TMA mice

Disulfiram (DSF, MedChemExpress, Monmouth Junction, NJ, USA) was administered via intraperitoneal injection (50 mg/kg) to C57BL/6N mice either 4 hours prior or 3 hours following CC injection, followed by sacrifice and analysis at 24 hours post-surgery. Control groups received an equivalent volume of solvent (10% dimethyl sulfoxide (DMSO)) without DSF at the corresponding time points.

Transcutaneous measurement of glomerular filtration rate

GFR measurements were performed in conscious mice 24 hours prior to and following crystalline TMA surgery.[3-5] In brief, the mice where anesthetized with isoflurane to mount a miniaturized imager device, consisting of two light-emitting diodes, a photodiode, and a battery (MediBeacon, Mannheim, Germany) onto the shaved neck of the mice. A background signal of the skin was recorded for 5 minutes. Following an intravenous injection of 150 mg/kg FITC-sinistrin (MediBeacon), each mouse was kept in an individual cage, and the signal was recorded for 90 minutes. The data analysis was performed using MPD Lab software (MediBeacon). GFR (µL/min) was calculated from the decrease of fluorescence intensity over time, using a three-compartment model, body weight, and an empirical

conversion factor.

Assessment of kidney infarct size

2,3,5-Triphenyltetrazolium chloride (TTC) staining was performed as previously described.[1,6] In brief, the harvested kidneys were sectioned and subjected to incubation with a 1% solution of TTC (Merck, Darmstadt, Germany) for 15 minutes at 37 °C. Subsequently, the sections were fixed in 4% formalin for 2 hours at room temperature, and the infarct size was quantified using Image J software (National Institutes of Health, USA).

Histological analysis

Kidney tissues were embedded in paraffin and sliced into 2 μm sections following PBS perfusion. Tubular injury was assessed using the Periodic acid-Schiff (PAS) reagent, and the degree of injury in ten images using a ×20 objective was scored based on the percentage of tubules displaying tubular cell necrosis, dilation, vacuolization, and infiltration of inflammatory cells. TdT-mediated dUTP-biotin nick end labeling (TUNEL)-positive kidney cell death (Roche, Mannheim, Germany) was quantified using Image J software by measuring the mean fluorescence intensity of five ×20 objective images. Immunohistochemistry was performed following endogenous peroxidase inhibition and heat-induced antigen retrieval. The sections were then blocked and incubated with primary antibodies including rabbit anti-gasdermin D (GSDMD, ab219800, Abcam, Cambridge, United Kingdom), rat anti-Ly6G (127601, BioLegend, Fell, Germany), mouse anti-alpha smooth muscle actin (αSMA, M0851, DAKO, Jena, Germany), and rabbit anti-fibrinogen (ab27913, Abcam). Diaminobenzidine was used for detection and images were captured using a Leica DMRBE microscope (Leica Microsystems, Wetzlar, Germany). Ly6G-positive area was quantified using Image J software by analyzing five images using a ×10 objective. Arterial occlusion was determined through the observation of fibrinogen staining within αSMA-positive arteries. Ten images were captured using a ×20 objective and scored on a 0-4 scale as follows: 0 = no occlusion, 1 = lesions in 1-25%, 2 = 25-50%, 3 = 50-75%, and 4 = 75-100%. Glomerular capillary thrombi were quantified as fibrinogen-positive area within the glomerulus using Image J software. This involved the analysis of six images from each kidney section, using a ×20 objective, where a minimum of ten glomeruli were collectively observed.

Immunofluorescence staining for murine samples

Kidney tissues were perfused with PBS, fixed with 4% paraformaldehyde for 2 hours, dehydrated in 30% sucrose for 24 hours, and then embedded in OCT compound (Sakura) and flash-frozen. The frozen specimens were sliced into sections with a thickness of 5 μm using a cryostat. The sections were blocked and incubated with primary antibodies, including rat anti-Ly6G (127601, BioLegend), mouse anti-αSMA (M0851, DAKO), rabbit anti-citrullinated histone 3 (CitH3, ab5103, Abcam), rabbit anti-CD41 (GTX113758, GeneTex, Irvine, CA, USA), and rat anti-TER-119 (116201, BioLegend). Subsequently, the sections were incubated with the specified secondary antibodies, and

mounted with 4',6-diamidino-2-phenylindole (DAPI)-containing medium (H-1200, Vector Laboratories, Newark, CA) and visualized under a confocal microscope (Zeiss LSM 800, Carl Zeiss, Oberkochen, Germany). The CitH3-positive area in the periinfarct was analyzed using Image J software by measuring the mean fluorescence intensity of ten ×20 objective images. The CitH3-positive, Ly6G-positive, CD41-positive, and Ly6G and CD41-positive area within αSMA-positive kidney arteries were scored on a 0-4 scale as follows: 0 = negative, 1 = lesions in 1-25%, 2 = 25-50%, 3 = 50-75%, and 4 = 75-100%, using ten 40× objective images.

MACSima imaging

Multiplex immunohistochemistry was performed on a MACSima imaging system (Miltenyi Biotec, Bergisch Gladbach, Germany). In brief, cyclic immunofluorescence imaging consisted of repetitive cycles of immunofluorescent staining, sample washing, multi-field imaging, and signal erasure by photobleaching. Cryosectioned slices of infarcted and sham-treat kidneys were placed on microscopy slides and fixed with acetone before the appropriate MACSWell™ imaging frame was mounted. Samples were preincubated with an antibody to CitH3 (ab5103, Abcam, 1:100 dilution, 4°C) overnight. Thereafter, nuclei were counterstained with DAPI and samples washed three times before being placed in the MACSima imaging system. Thereafter a total of 23 antibodies were stained and recorded in 11 MACSima imaging cycles according to the table below. DAPI was added in the 8th cycle to renew nuclear staining.

Cycle	Dilution	Antigen	Clone	Company	Order number	Fluorochrome
1	1:500	Rabbit IgG	Polyclonal	Miltenyi	130-123-564	APC
1	1:50	Ki67	REA183	Miltenyi	130-117-691	FITC
1	1:50	Ly6G	1A8	Miltenyi	130-123-712	PE
2	1:50	CD169	3D6.112	Biolegend	142406	FITC
2	1:50	CXCR2	SA044G4	Biolegend	149304	PE
3	1:50	Ter119	TER_119	Biolegend	116206	FITC
3	1:50	CXCR4	REA107	Miltenyi	130-118-682	PE
4	1:50	CD11b	M1/70	Miltenyi	130-115-988	APC
4	1:50	CD45	REA737	Miltenyi	130-110-796	FITC
4	1:50	Ly6C	REA796	Miltenyi	130-111-916	PE
5	1:50	MHCII	REA813	Miltenyi	130-112-229	FITC
5	1:50	Sca1	D7	Biolegend	108107	PE
6	1:50	CD45R	RA3-6B2	Miltenyi	130-118-462	FITC
6	1:50	CD41	REA1194	Miltenyi	130-122-760	PE
7	1:10	CD115	AFS98	Miltenyi	130-102-504	APC
7	1:50	SMA	REAL650	Miltenyi	130-123-363	FITC
7	1:50	CD61	REA1192	Miltenyi	130-122-148	PE
8	1:50	Cleaved caspase 3	D3E9	Cell Signaling	9603	FITC
8	1:50	F4/80	REA126	Miltenyi	130-116-499	PE
9	1:50	CD19	REA749	Miltenyi	130-111-883	PE
10	1:10	CD68	FA-11	Miltenyi	130-102-918	APC
10	1:10	CD3e	17A2	Miltenyi	130-117-785	PE

11	1:50	CD31	REAL260	Miltenyi	130-118-936	PE

Acquired pictures were stitched and preprocessed using MACS iQ View Analysis Software (Miltenyi Biotec) and representative overlay pictures displayed.

Flow cytometry of murine kidney, spleen, lung, bone marrow, and blood

Kidney, spleen, lung, bone marrow and peripheral blood were collected and single-cell suspensions were prepared as previously described.[7-9] Briefly, kidneys were mashed and incubated with collagenase (Sigma-Aldrich) and deoxyribonuclease I (Roche) for 40 minutes at 37°C. The digested tissues were filtered through 23- and 25-gauge needles, followed by 70 μm and 30 μm strainers. Spleens and lungs were directly filtered through 70 μm and 30 μm strainers using the end of a syringe. Bone marrow was flushed from femurs and filtered through 70 μm strainers. Ammonium chloride solution was used to remove the red blood cells in spleen, bone marrow and blood. The cells were then suspended in wash buffer (2% fetal calf serum (FCS) in PBS), treated with Fc receptor blocker, and stained with the following antibodies: PE or APC anti-CD45, FITC anti-CD11b (MAC-1) (BD Biosciences, Heidelberg, Germany), PerCP or FITC anti-Ly6G (BioLegend), APC anti-Ly6C (BioLegend), PE anti-CD101 (Thermo Fisher Scientific, Waltham, MA, USA), PerCP/Cyanine5.5 anti-CXCR2 (BioLegend), and rabbit anti-CitH3 (Abcam) followed by APC anti-rabbit IgG (Thermo Fisher Scientific). Caspase1 activation was detected using Pyroptosis/Caspase-1 Assay Green (9145, ImmunoChemistry, Bloomington, MN, USA). Flow cytometry was performed on a FACSCalibur (Becton Dickinson, New Jersey, USA), and data were analyzed using the FlowJo version 10 software (Tree Star, Ashland, OR, USA). AccuCheck counting beads (Thermo Fisher Scientific) were used to determine the absolute cell counts according to manufacturer's instruction.

NETs measurement in murine kidney

NETing neutrophils, which are undergoing NETosis, were identified in kidney by flow cytometry as CitH3+ cells among CD45+ CD11b+ Ly6G+ neutrophils, as previously described.[10,11] The absolute number was determined using AccuCheck counting beads (Thermo Fisher Scientific).

Measurement of IL-1β and histone in murine plasma

The levels of IL-1β in mouse plasma were measured using mouse IL-1β sandwich enzyme-linked immunosorbent assay (ELISA) kit (Proteintech, Rosemont, IL, USA). The levels of circulating histone were quantified as histone-DNA complexes through Cell Death Detection ELISA Plus (Roche).

Immune cell isolation from murine kidney

Kidney tissues were perfused with PBS, minced into small pieces, and subsequently incubated with collagenase (Sigma-Aldrich) and deoxyribonuclease I (Roche) for 1 hour at 37°C. The digested tissues were filtered through 70 μm strainers and subjected to centrifugation. The cells were resuspended in a 70% Percoll solution, overlaid with 37% Percoll, followed by 30% Percoll solutions

to establish a density gradient. After centrifugation at 900g for 30 minutes at room temperature, the cell layer at the 70%-37% interface was collected as the immune cell fraction. The cells were washed and proceeded to immunoblot analysis.

Immunoblotting

Total protein from kidney tissues or cells was extracted in RIPA buffer (Thermo Fisher Scientific), which was supplemented with protease and phosphatase inhibitors (Thermo Fisher Scientific). Insoluble components were removed by centrifugation at 12000g for 10 minutes, and protein concentration was determined by Bradford assay (Bio-rad, Hercules, CA, USA). Protein was denatured using Laemmli buffer and 2-mercaptoethanol, and boiled for 5 minutes at 95°C. For the cleavage study, cell culture supernatants were precipitated using methanol chloroform extraction method as previously described.[12] In brief, an equal volume of methanol and 0.25 volumes of chloroform were added, vortexed, and centrifuged for 10 minutes at 20,000g. The upper phase was discarded, and 500 µL of methanol was added to the interphase. This mixture was centrifuged for 10 minutes at 20,000g, and the protein pellet was dried at 55°C, resuspended in Laemmli buffer with 2-mercaptoethanol, and boiled for 5 minutes at 95°C. Samples were separated by 10% SDS-PAGE and were transferred to PVDF membranes. The following primary antibodies were used: anti-mouse caspase-1 (AG-20B-0042-C100, Adipogen, San Diego, CA, USA), anti-human GSDMD (#69469, Cell Signaling Technology, Danvers, MA, USA), anti-mouse GSDMD (ab219800, Abcam), anti-human/mouse IL-1β (#12242, Cell Signaling Technology), and anti-β actin (#4967, Cell Signaling Technology). The following secondary antibodies were used: anti-rabbit IgG-HRP (#7074, Cell Signaling Technology) and anti-mouse IgG-HRP (#7076, Cell Signaling Technology). The blot was visualized using an ECL substrate on a ChemiDoc Imaging System (Bio-Rad).

iPS cell culture and generation of neutrophil granulocytes

Healthy control fibroblast derived induced pluripotent stem (iPS) cells were kindly provided from Dr. Drukker (Institute of Stem Cell Research and the Induced Pluripotent Stem Cell Core Facility, Helmholtz Center Munich). Undifferentiated iPS cell colonies were disseminated on 6-well culture plates coated with growth factor-reduced matrigel (Becton-Dickinson, cat# 356230) in mTeSR1 medium. BMP4 (80 ng/mL, Peprotech cat# 120-05), CHIR99021 (4 µM, millipore cat# 361571) and VEGF (80 ng/mL, Peprotech cat# 100-20) were added to the medium on day 0 of differentiation. On day 2, medium was replaced by essential 6 medium (Thermo Fisher scientific, cat# A1516401) supplemented with VEGF (80 ng/mL), basic FGF (25 ng/mL, Peprotech cat# 100-18B), SCF (50 ng/mL, Peprotech cat# 300-07) and SB431542 (2 µM, selleckchem cat# S1067). The cytokines were switched to SCF (50 ng/mL), IL-3 (50 ng/mL, Peprotech cat# 200-03), Flt-3 (50 ng/mL, Peprotech cat# 300-19), TPO (5 ng/mL, Peprotech cat# 300-18) and VEGF (50 ng/mL) with StemPro-34 SFM medium (Thermo Fisher scientific, cat# 10639011) on day 6 for hemangiogenic progenitor cells. On day 8, medium was replaced by StemPro-34 SFM medium supplemented with SCF (50 ng/mL), IL-3 (50 ng/mL), Flt-3 (50 ng/mL), TPO (5 ng/mL) and doxycycline (0.05 µg/mL). Thereafter, half

medium was changed every 3-4 days until day17. On day17, cytokines were changed to G-CSF (50 ng/mL, Peprotech cat# 300-23), SCF (50 ng/mL), IL-3 (50 ng/mL). Mature neutrophil-like cells appeared around day 20 after differentiation. Floating live cells were enumerated upon Trypan blue staining in a counting chamber.

Immunofluorescence sample preparation for iPS cells

For immunofluorescence, cells were centrifuged at 500 rpm for 5 minutes using a Tharmac Cellspin I Cytocentrifuge onto air-dried slides. Cells were fixed with 4% paraformaldehyde, followed by staining and visualization using confocal microscope.

sgRNA design

sgRNA-Cas9 with fusion GFP plasmid was purchased from Addgene (PX458, cat#48138). sgRNAs targeting Gasdermin D target 1 (ACTTCTACGATGCCATGGAT), and Gasdermin D target 2 (CAGCGAGTACACATTCATTG) genes were designed with the online CRISPR Design tool developed by Feng Zhang's Lab (http://crispr.mit.edu/). sgRNA with a lower number of predicted potential off target sites in coding region were selected. sgRNA-Cas9 vector and single-stranded oligodeoxynucleotide (ssODN, bought from Integrated DNA Technologies, IDT) were co-transfected into healthy control-derived iPS cells using Amaxa Nucleofector® II Device (Lonza, program B-016) using Human stem cell nucleofector kit 2 (Lonza, cat# VPH-5022). pCas-Guide vector with a scrambled sequence was used as control. Two days after transfection, GFP positive cells were sorted by BD FACS Aria (BD Biosciences) and 3000 iPS cells were seeded on a 10cm dish pre-coated with mouse embryonic fibroblasts. 10 days after seeding, each colony derived from a single cell was picked up for genotyping and further expansion. Genotyping primers are as follows:
GCTCTGCAGCCTCTAGCTC
GTTCCGGCCACAGCGCTC

Polymerase chain reaction (PCR) and Sanger sequencing

Each PCR reaction comprised 15.3 μL of deionized water, 2.5 μL or 10x ThermoPol reaction buffer (New England Biolabs, Ipswich, MA, USA), 4 μL of 1.25 mM dNTP, 1 μL of each primer (10 μM), 0.2 μL of Taq DNA polymerase (New England Biolabs), and 1 μL of DNA sample. For the amplification of GSDMD DNA, PCR was performed using the GeneTouch Plus Thermal Cycler (Biozym Scientific, Oldendorf, Germany) under the following conditions: initial denaturation at 94 °C for 3 minutes, followed by 35 cycles of denaturation at 94 °C for 40 seconds, annealing at 62 °C for 45 seconds, and extension at 72 °C for 60 seconds. A final extension step was performed at 72 °C for 5 minutes. The PCR product was mixed with 5 μl of loading dye and electrophoresed in a 2% agarose gel containing peqGREEN dye (Peqlab, Erlangen, Germany) at 200 V for 20 minutes, followed by visualization under UV light. Upon confirmation of the targeted amplification, the product underwent purification using ExoProStar (GE Healthcare Life Sciences, Marlborough, MA, USA) and was submitted to Eurofins Genomics (Ebersberg, Germany) for Sanger sequencing. The

obtained sequencing data were analyzed using DNASTAR software (Madison, WI, USA).

Human neutrophil stimulation for inflammasome assays

Human blood neutrophils were suspended in Hanks' Balanced Salt Solution (HBSS) supplemented with 2% FCS and seeded on a 24-well plate at a density of 5×10^5 cells/mL for interleukin (IL)-1β and lactate dehydrogenase (LDH) measurement, and 3×10^6 cells/mL for immunoblot analysis. The cells were primed with 100 ng/mL of lipopolysaccharide (LPS) for 2 hours. After pretreatment with or without DSF (35-50 μM, MedChemExpress), VX-765 (50 μM, InvivoGen, San Diego, CA, USA), necrostatin-1s (Nec-1s, 50 μM, Selleck, Houston, TX, USA), necrosulfonamide (NSA, 15 μM, MedChemExpress), and anakinra (100-1000 ng/mL, Sobi, Stockholm, Sweden) for 1 hour, the cells were stimulated with CC or nigericin (10 μM, InvivoGen) for 3 hours under shaking conditions. Following incubation, cell-free supernatants were harvested for IL-1β ELISA (Invitrogen, Waltham, MA, USA) and LDH assay (Roche). Cell-free supernatants and cell lysates from 3 wells were combined for each condition and subsequently used for immunoblot analysis.

iPSC-derived neutrophil stimulation for inflammasome assays

iPS cell (iPSC)-derived neutrophils were suspended in HBSS supplemented with 2% FCS, and seeded on a 96-well plate at a density of 6.7×10^5 cells/mL. The cells were primed with 100 ng/mL of LPS for 4 hours, followed by stimulation with CC (1.5 mg/mL) or nigericin (10 μM, InvivoGen) for 3 hours under shaking conditions. Following incubation, cell-free supernatants were collected for IL-1β ELISA (Invitrogen) and LDH assay (Roche).

Human neutrophil and iPSC-derived neutrophil stimulation for NETs analysis

Human neutrophils or iPSC-derived neutrophils were suspended in HBSS supplemented with 2% FCS and seeded at a density of 2×10^6 cells/mL in 1.5 mL Eppendorf tubes for SYTOX Green (SG) flow cytometric analysis, or 8-well chamber slides precoated with CC (4 mg/mL) for immunofluorescent and live cell imaging. The cells were primed with CXCL8 (10 ng/mL, Immunotools, Friesoythe, Germany) for 30 minutes and then treated with or without DSF (35-50 μM, MedChemExpress), diphenyleneiodonium chloride (DPI, 10 μM, Sigma-Aldrich), or DMSO for 1 hour. The cells were stimulated with CC (only added for flow cytometric analysis), phorbol 12-myristate 13-acetate (PMA, 20 nM, Sigma-Aldrich), or histone (100 μg/mL, Sigma-Aldrich) for 3 hours for flow cytometric analysis, and 4 hours for immunofluorescent and live cell imaging.

Quantification of SYTOX Green positive neutrophils by flow cytometry

The cells were stained with SG (20 nM, BioLegend) and immediately analyzed by flow cytometry using a FACSCalibur (Becton Dickinson). The data were analyzed using the FlowJo version 10 software.

Live cell imaging with SYTOX Green

The cells were stained with SG (5 μM, BioLegend) and immediately visualized using a confocal microscope (Zeiss LSM 800).

Immunofluorescence staining for cells

Cells were fixed with 4% paraformaldehyde for 10 minutes and permeabilized for 5 minutes using 0.2% TritonX-100. Subsequently, the cells were blocked and incubated with primary antibodies, including rabbit anti-GSDMD (69469S, Cell Signaling Technology), rabbit anti-CitH3 (ab5103, Abcam), and mouse anti-myeloperoxidase (MPO) (ab25989, Abcam). The cells were then incubated with the specified secondary antibodies, and mounted using medium containing DAPI (H-1200, Vector Laboratories). Confocal microscopy was performed using a Zeiss LSM 800 microscope.

β_2 integrin activation assay for iPSC-derived neutrophils

β_2 integrin activation assay was performed on iPSC-derived neutrophils as previously described.[7] Briefly, iPSC-derived neutrophils were suspended at a density of 3.3×10^5 cells/mL in HBSS buffer, containing 0.1% glucose, 1 mM $CaCl_2$, 1 mM $MgCl_2$, 0.25% BSA, and 10 mM HEPES, followed by stimulation with CXCL8 (100 ng/mL, Immunotools) for 10 minutes at 37°C. The activation was then stopped by adding ice-cold wash buffer (2% FCS in PBS). Surface expression levels of β_2 integrins were quantified using Alexa Fluor 488 anti-CD11a/CD18 (LFA-1) and PerCP anti-CD11b (MAC-1) antibodies (both from BioLegend) via flow cytometry on a FACSCalibur (Becton Dickinson). The data were analyzed using FlowJo version 10 software.

Isolation of mouse bone marrow neutrophils

Mouse bone marrow neutrophils were isolated by negative MACS selection with the Neutrophil Isolation Kit (Miltenyi Biotec) according to the manufacturer's instructions.

Mouse neutrophil stimulation for NETs analysis

Mouse bone marrow neutrophils were suspended in HBSS supplemented with 1% FCS and seeded at a density of 1.5×10^6 cells/mL in 1.5 mL Eppendorf tubes for SG flow cytometric analysis, or 8-well chamber slides precoated with CC (4 mg/mL) for immunofluorescent and live cell imaging. The cells were stimulated with CC (1.0 mg/mL, for flow cytometric analysis) or histone (100 μg/mL, Sigma-Aldrich) for 3 hours for flow cytometric analysis, and 4 hours for immunofluorescent and live cell imaging.

Bone marrow cell culture and stimulation for maturation analysis

Mouse bone marrow cells were suspended in RPMI 1640 supplemented with 10% FCS and seeded on a 24-well plate at a density of 8×10^5 cells/mL. Cells were incubated with or without granulocyte colony-stimulating factor (G-CSF, 100 ng/mL, Immunotools) or tumor necrosis factor alpha (TNFα, 20 ng/mL, Immunotools) for 24 hours. Surface expression levels of CXCR2 within mature neutrophils (Ly6G+ CD101+) were quantified as mean fluorescence intensity using flow cytometry

(FACSCalibur, Becton Dickinson). The data were analyzed using FlowJo version 10 software.

Flow chamber experiments

The flow adhesion assay was performed using a flow chamber system (Maastricht Instruments, Maastricht, Netherlands). Coverslips were coated with type I collagen (50 µg/mL) and subsequently blocked with 1% BSA. Heparinized mouse whole blood samples were diluted in Tyrode's buffer containing 2 mM $CaCl_2$ and incubated with CC (2.5 mg/mL) or PBS 1X for 10 minutes at 37°C. The samples were then perfused over collagen-coated coverslips at a shear rate of 1000 s^{-1}. Afterward, the flow chamber system was washed with Tyrode's buffer without $CaCl_2$. A second step flow adhesion assay was performed by perfusing mouse bone marrow neutrophils (2.5×10^6 cells per sample, pre-stained with RedDeep Cell tracker dye (Invitrogen)) through the chamber at a shear rate of 500 s^{-1} over platelet-rich thrombi. Slides were fixed with 4% paraformaldehyde for 10 minutes, then blocked with 2.5 % BSA and incubated overnight with primary antibodies, including rabbit anti-CitH3 (ab5103, Abcam) and rat anti-CD41 (ab33661, Abcam). Next days, the slides were washed with PBS 1X, then incubated with specified secondary antibodies, and mounted using medium containing DAPI (H-1200, Vector Laboratories). Ten pictures were taken for each condition using confocal fluorescence microscope (Zeiss LSM 800, Oberkochen) and 63x objective. Quantification of immunofluorescence signals was obtained using Fiji ImageJ software and the analyze particle module.

Primary renal tubular cell isolation and cell death assay

Primary renal tubular cell isolation was performed as previously described.[8,13] Briefly, the kidneys harvested from 3 to 4-week-old mice were mashed and incubated with collagenase D (1.5 mg/mL) for 30 minutes at 37°C. The digested kidney tissue was then filtered through 20- and 25-gauge needles, followed by filtration through a 70 µm strainer. The red blood cells were removed using ammonium chloride solution. The cell suspensions were layered onto 31% Percoll solution and then centrifuged at 3000 rpm for 15 minutes at 4°C. The cells were subsequently resuspended and cultured with predefined K1 medium.[13] The cultured cells were seeded at a density of 1×10^5 cells/mL in a 96-well plate. After overnight incubation, the cell culture media were replaced with K1 medium without FCS, and then the cells were treated with 1 mM H_2O_2 to simulate hypoxia-induced cell death. Cell-free supernatants were collected after 24 hours and subjected to LDH assay (Roche). For time-lapse analysis, the cells were stained with SG (0.5 µM, BioLegend), and time-lapse images were obtained every 30 minutes for 24 hours using a Nikon Eclipse Ti2 microscope (NIKON, Tokyo, Japan). The SG-positive area in each time point was quantified by NIS-Elements Viewer software (NIKON).

Analysis of single cell RNA sequencing

An analysis of single-cell RNA sequencing (scRNA-seq) was performed utilizing a previously published dataset[14] that contained cells from the kidney, blood, and spleen of C57BL/6J mice. The cells were sorted before and after 45 minutes of unilateral kidney ischemia followed by reperfusion for 1 and 3 days. For scRNA-seq, a 1:1 mixture of CD11b+ cells and F4/80+ cells from the kidney

sample, a 1:1 mixture of CD11b+ cells and Ly6C+ cells from the blood samples, and the CD11b+ cells from the spleen samples at each time point were loaded onto 10X Genomics. For quality control, cells with mitochondrial gene percentages less than 50%, unique gene counts between 1,000 to 50,000, and detected genes between 200 to 7,000 were kept. The normalization of the data was conducted using the scran package,[15] which included assuming equal size factors, normalizing the library size to counts per million, and log-transforming the count data. Principal component analysis was performed based on the 4,000 highly variable genes. To eliminate technical differences and preserve biological differences, the harmony integration pipeline was employed, which reduces data dimensions and removes batch effects.[16] The reduction of data dimensions and Uniform Manifold Approximation and Projection (UMAP) was applied for unsupervised clustering based on the first 50 integrated principal components. For the clustering of the mononuclear phagocytic cell subset and neutrophil subset, the resolution was set to 1 and 0.5 respectively. The gene enrichment score was evaluated by "scanpy.tl.score_genes()" functions.[17] A total of 26 clusters were identified among the 80,829 cells that passed quality control. Clusters 3 and 15 were identified as neutrophils based on the expression of representative neutrophil-related genes (Ltf, Ngp, Ly6g, Mmp8, Gm5483, Stfa2l1, Cxcl2, Il1b) (Supplementary figure S1A) and were further categorized into 8 clusters (G0-4 and G5a-c) based on their differentiating and maturation stages, as described in a previous report (Table 1).[18] GM cells, which are low-quality G3-like cells with a low unique molecular identifier (UMI) count per cell and per gene and a high percentage of mitochondrial UMI counts, were excluded from all analyses.

Data Sharing Statement

Data are available upon reasonable request to the corresponding author.

Supplementary Tables

Supplementary table S1. Categorization of neutrophil subpopulations based on differential gene expression

G0	G1	G2	G3	G4
Rpl12	Elane	Chil3	Ltf	Retnlg
Rps20	Prtn3	Tuba1b	Ngp	Mmp8
Npm1	Mpo	2810417H13Rik	Camp	S100a6
Hsp90ab1	Ms4a3	Camp	Ifitm6	Prr13
Rpl10a	Nkg7	Stmn1	Chil3	S100a9
Rpl3	Rps2	Hmgn2	Lcn2	Wfdc21
Rpsa	Plac8	Ngp	Ly6g	S100a8
Ptma	mt-Nd1	H2afz	Cybb	Lgals3
Rps18	Rpl3	Tubb5	AA467197	Mgst1
Rps19	Rpl12	Ppia	Anxa1	Ly6g
Rplp1	Ptma	Ptma	Cd177	Ly6c2
mt-Nd1	Rps18	Anp32b	Wfdc21	Cd177
mt-Nd2	mt-Atp6	Cebpe	Serpinb1a	Ceacam10
Rps17	Rpl10a	Hmgb2	Adpgk	Adpgk
Rps12	Rps17	Serpinb1a	Dstn	Capg
Rps2	Rps19	H2afv	Itgb2l	Thbs1
Rpl32	Rpl36a	Tuba4a	Ltb4r1	Mrgpra2b
Rps8	Rpsa	Hmgb1	Lyz2	Cxcl2
Rps5	Rpl32	Birc5	Cpne3	
Rpl36a	Rps20	Smc4	Anxa3	
Rps4x	Rps12	Top2a	Capg	
Rpl14	Rps8	H2afx	Aldh2	
Gnb2l1	Rps4x	Fcnb	Ly6c2	
mt-Atp6	Rpl35	Smc2	Cebpe	
Rpl28	Rpl14	Dek	St3gal5	
Xist	mt-Cytb	Mki67	Mgst2	
Hsp90aa1	mt-Co3	Rrm2	Syne1	
Rpl22	Ctsg	Ube2c	Lta4h	
Rpl35	Gstm1	Nusap1	Zmpste24	
H2afy	Calr	Hist1h2ap	Orm1	

G5a	G5b	G5c	GM
Ccl6	Isg15	Il1b	mt-Co1
Clec4d	Rtp4	Lst1	mt-Co3
Dusp1	Rsad2	Ifitm2	mt-Atp6
Fos	Ifitm3	Rps27rt	mt-Co2
Fxyd5	Oasl2	Csf3r	mt-Cytb
Btg1	Ly6e	Tsc22d3	mt-Nd4
Grina	Ifit3	Btg1	mt-Nd1

Il1b	Ifit3b	Dusp1	Ifitm6
Ctsd	Ifi27l2a	Fgl2	Ltf
Fth1	Gm13822	Cst3	Wfdc21
Csf3r	Ifit1	Pla2g7	mt-Nd2
Amica1	Irf7	Gm2a	Camp
Ypel3	Slfn4	Ifitm1	Ngp
Hbb-bs	Trim30a	Cdk2ap2	Cybb
Sirpb1b	Slfn1	Sirpb1b	Cd177
Sell	Fgl2	1600010M07Rik	Lcn2
Mcl1	Ifi204	H2-Q10	Anxa1
Arg2	H2-T23	Txnip	Chil3
H2-Q10	Oasl1	Cxcr4	Adpgk
Cyp4f18	Stat1	Gngt2	Dstn
Klf2	Isg20	Wfdc17	AA467197
Il1f9	Cmpk2	Rnf149	Itgb2l
Slc16a3	Slfn5	Marcks	Cpne3
Gm10116	Oas3	Ninj1	Syne1
Fosl2	Usp18	Sirpb1c	Ckap4
Creg1	Irgm1	Tnfaip2	Golim4
Gm5483	Zbp1	Hbb-bs	Gm42418
Rdh12	Xaf1	Adgre5	mt-Nd3
Stfa2l1	Ifi47	Ptafr	C3
Asprv1	Gbp2	Hba-a1	Thbs1

Supplementary Figures

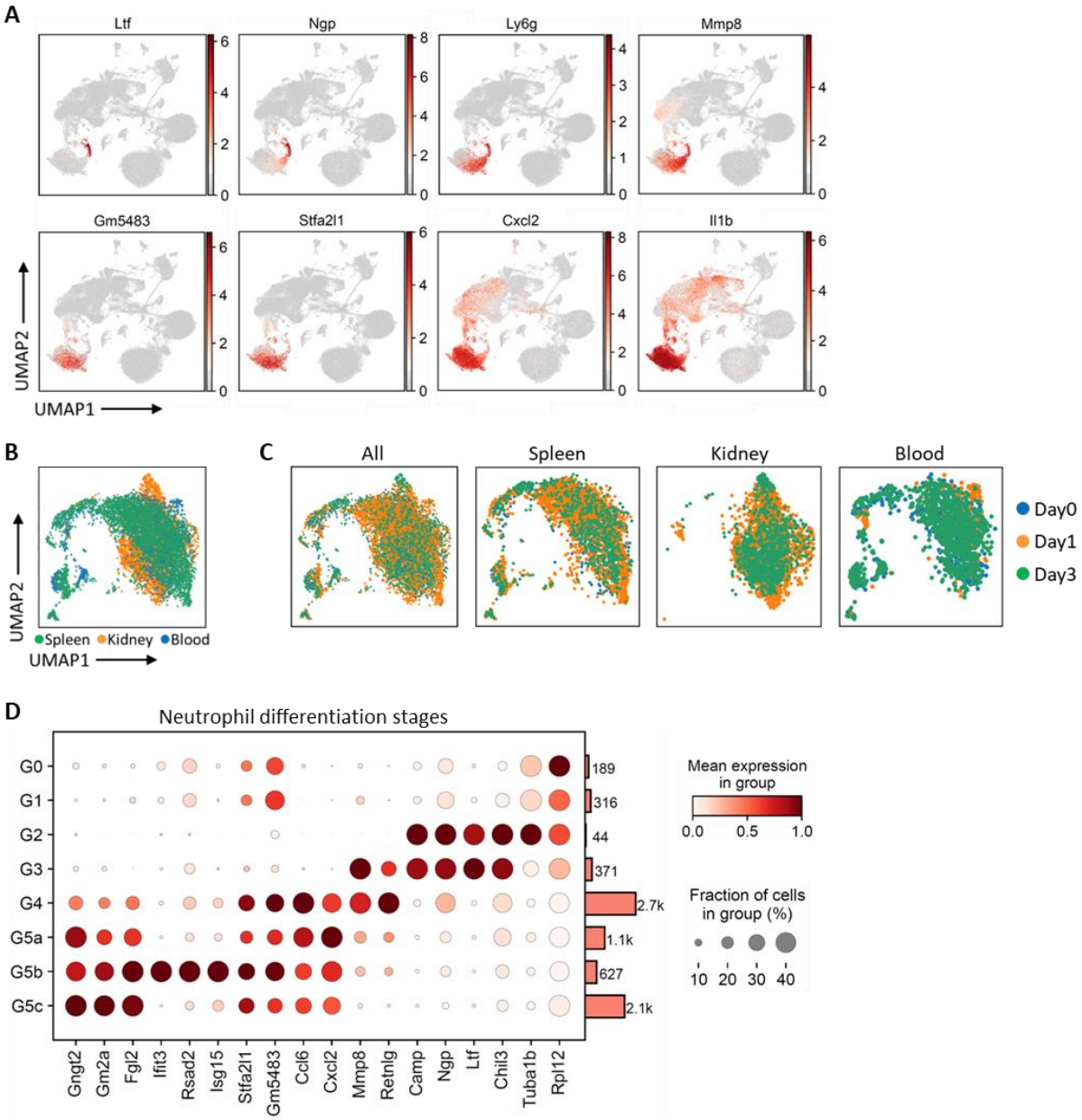

Supplementary figure S1. Identification of neutrophil populations in scRNA-seq data sorted from the kidney, blood, and spleen of C57BL/6J mice on day 0, 1, and 3 after uIRI

A) Characteristic plots of representative genes expressed in neutrophils.

B) Uniform Manifold Approximation and Projection (UMAP) plot of the distribution of neutrophils clusters, colored by sample origin, at all time points.

C) UMAP plot of neutrophil clusters exhibiting different time points in each organ.

D) Dot plot representing the expression profile of representative neutrophil marker genes for each cluster. The dot color indicates the average gene expression level in each cluster, while the dot size represents the percentage of cells in each cluster.

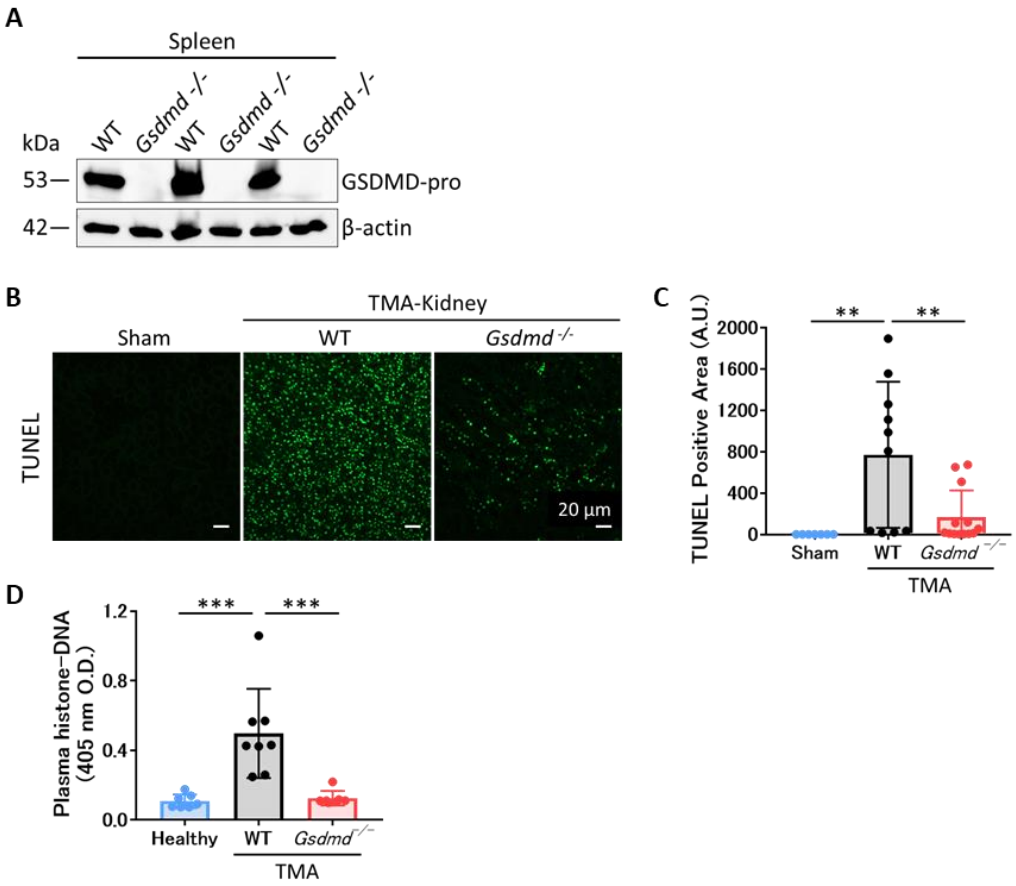

Supplementary figure S2. ***Gsdmd*-deficiency reduced the levels of circulating histone following focal crystalline TMA**

A) Immunoblot analysis of gasdermin D (GSDMD) in spleens of three sets of wild-type (WT) and *Gsdmd*$^{-/-}$ mice. β-actin was used as a loading control.

B) Representative images of TdT-mediated dUTP-biotin nick end labeling (TUNEL) staining on sham and thrombotic microangiopathy (TMA) kidneys of WT and *Gsdmd*$^{-/-}$ mice.

C) Quantification of the TUNEL-positive kidney cell death area of sham (n=7) and TMA kidneys from WT (n=10) and *Gsdmd*$^{-/-}$ (n=13) mice.

D) The levels of circulating histone in healthy mice (n=7) and focal TMA mice (WT: n=8, *Gsdmd*$^{-/-}$: n=7) quantified by ELISA.

Scale bars: (B) 20 μm. The data represent means ± SD. **$p < 0.01$ and ***$p < 0.001$ using one-way ANOVA with Tukey's post-hoc test.

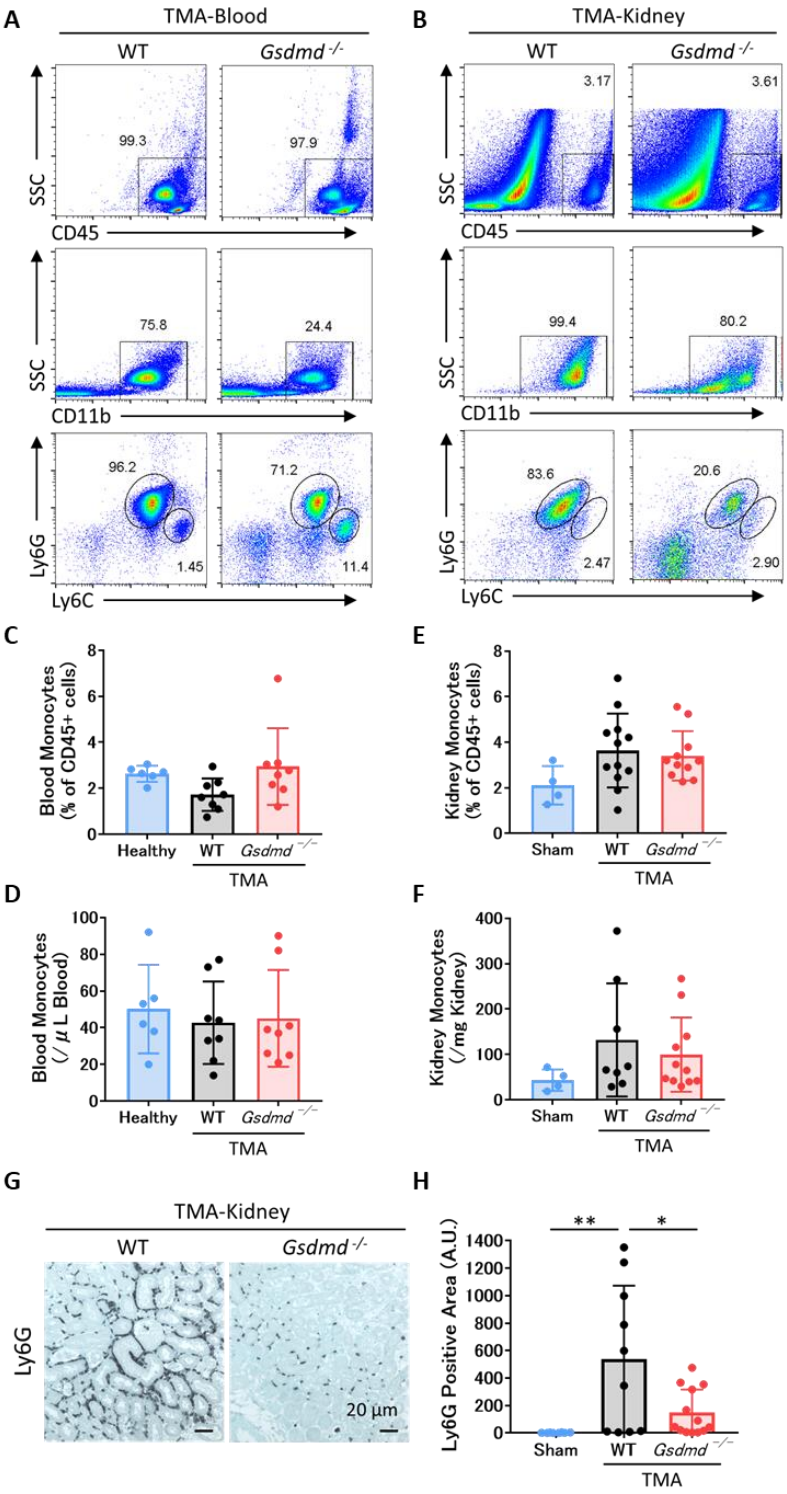

Supplementary figure S3. Gating strategy for identifying neutrophils and monocytes in blood and kidney of focal TMA mice

A)-B) Representative images of the gating strategy for identifying neutrophils (CD45+ CD11b+ Ly6G+) and monocytes (CD45+ CD11b+ Ly6C+) in blood (A) and kidney (B) from wild-type (WT) and gasdermin D knockout (*Gsdmd*$^{-/-}$) mice with focal thrombotic microangiopathy (TMA).

C)-D) Percentage of monocytes among CD45+ cells (D) and their absolute number (E) in blood from healthy mice (n=6) and focal TMA mice (WT: n=8, *Gsdmd*$^{-/-}$: n=8).

E)-F) Percentage of monocytes among CD45+ cells (F) and their absolute number (G) in sham (n=4) and TMA kidneys from WT (n=8-12) and *Gsdmd*$^{-/-}$ (n=11) mice.

G) Representative immunohistochemical images of Ly6G staining on kidneys.

H) Quantification of Ly6G-positive area in sham (n=8) and TMA kidneys from WT (n=10) and *Gsdmd*$^{-/-}$ (n=13) mice.

Scale bars: (G) 20 μm. The data represent means ± SD. *$p < 0.05$ and **$p < 0.01$ using one-way ANOVA with Tukey's post-hoc test.

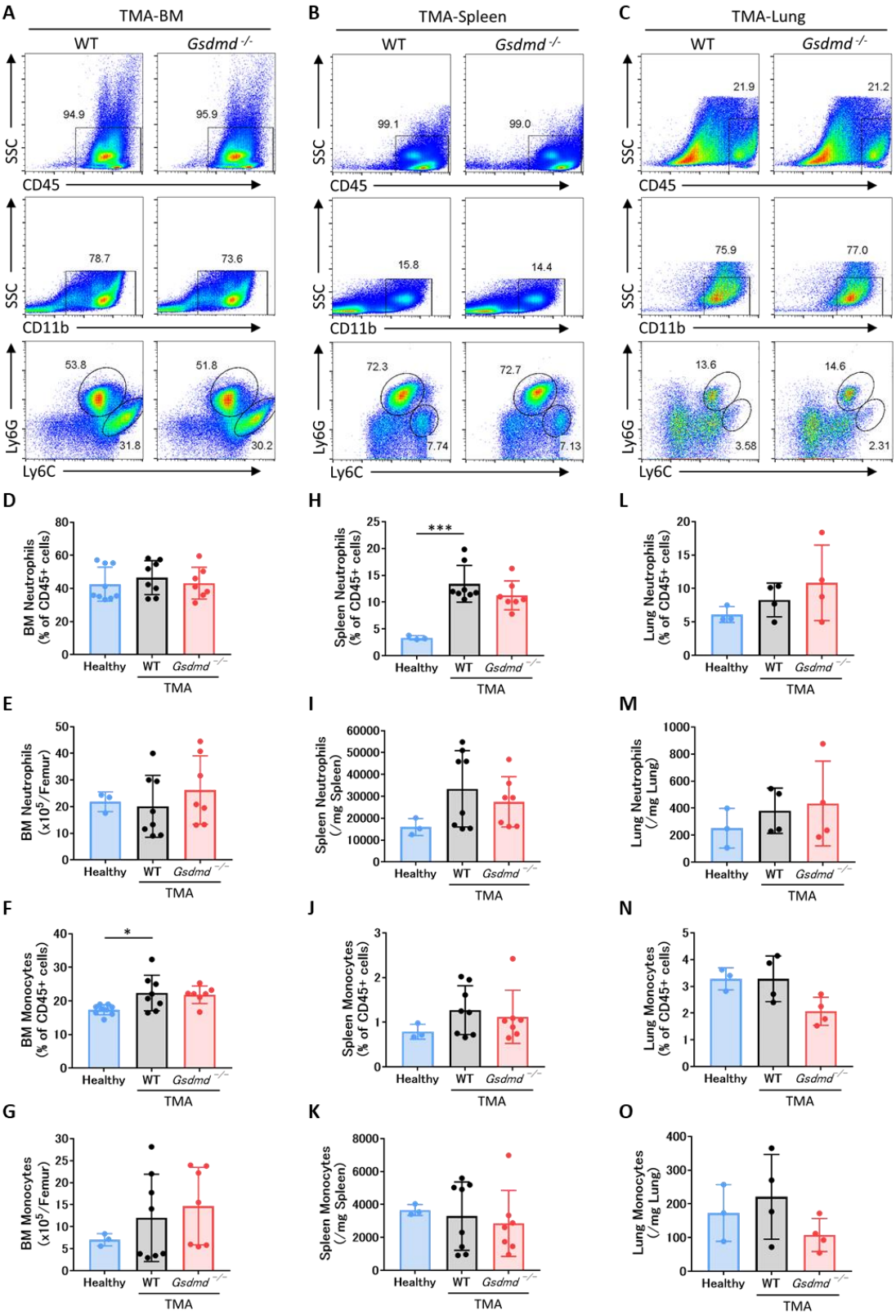

Supplementary figure S4. ***Gsdmd*-deficiency did not alter the number of neutrophils and monocytes in the bone marrow, spleen, and lung following focal crystalline TMA**

A)-C) Representative images of the gating strategy for identifying neutrophils (CD45+ CD11b+ Ly6G+) and monocytes (CD45+ CD11b+ Ly6C+) in bone marrow (BM) (A), spleen (B), and lung (C) from wild-type (WT) and gasdermin D knockout (*Gsdmd*$^{-/-}$) mice following cholesterol crystal (CC)-induced thrombotic

microangiopathy (TMA).
D)-E) Percentage of neutrophils among CD45+ cells (D) and their absolute number (E) in BM from healthy mice (n=3-9) and focal TMA mice (WT: n=8, *Gsdmd*$^{-/-}$: n=7).
F)-G) Percentage of monocytes among CD45+ cells (F) and their absolute number (G) in BM from healthy mice (n=3-9) and focal TMA mice (WT: n=8, *Gsdmd*$^{-/-}$: n=7).
H)-I) Percentage of neutrophils among CD45+ cells (H) and their absolute number (I) in spleen from healthy mice (n=3) and focal TMA mice (WT: n=8, *Gsdmd*$^{-/-}$: n=7).
J)-K) Percentage of monocytes among CD45+ cells (J) and their absolute number (K) in spleen from healthy mice (n=3) and focal TMA mice (WT: n=8, *Gsdmd*$^{-/-}$: n=7).
L)-M) Percentage of neutrophils among CD45+ cells (L) and their absolute number (M) in lung from healthy mice (n=3) and focal TMA mice (WT: n=4, *Gsdmd*$^{-/-}$: n=4).
N)-O) Percentage of monocytes among CD45+ cells (N) and their absolute number (O) in lung from healthy mice (n=3) and focal TMA mice (WT: n=4, *Gsdmd*$^{-/-}$: n=4).
The data represent means ± SD. *$p < 0.05$ and ***$p < 0.001$ using one-way ANOVA with Tukey's post-hoc test.

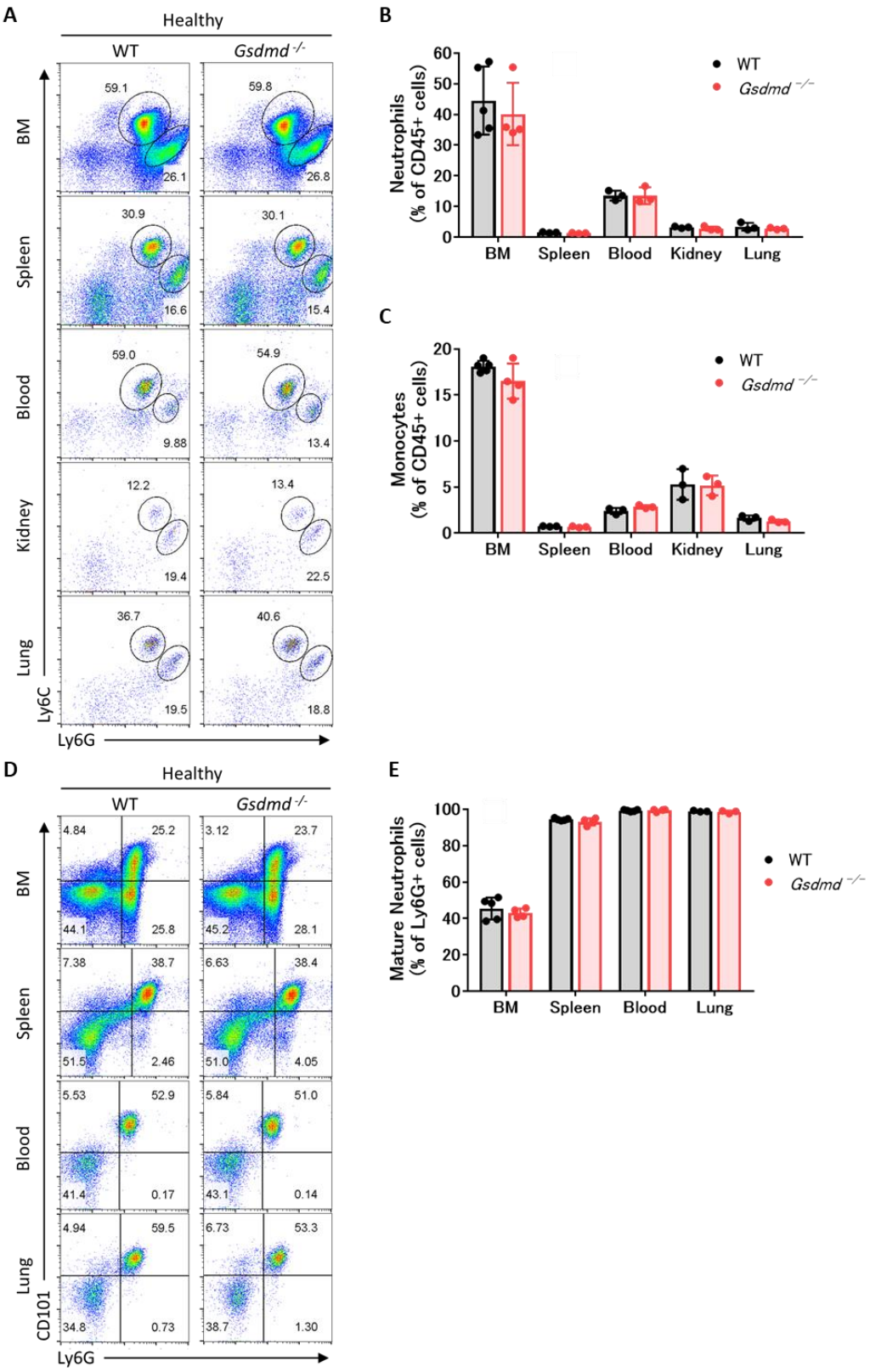

Supplementary figure S5. No difference in the number and maturation of neutrophils between WT and *Gsdmd*$^{-/-}$ mice under normal conditions

A) Representative gating of flow cytometric analysis for the quantification of neutrophils (CD45+ CD11b+ Ly6G+) and monocytes (CD45+ CD11b+ Ly6C+) in bone marrow (BM), spleen, blood, kidney, and lung from wild-type (WT) and gasdermin D knockout (*Gsdmd*$^{-/-}$) mice in a healthy state.

B)-C) Percentage of neutrophils (B) and monocytes (C) among CD45+ cells in each organ (n=3-5 per group).
D) Representative gating of flow cytometric analysis for the quantification of mature neutrophils (CD45+ CD11b+ Ly6G+ CD101+) in BM, spleen, blood, and lung from WT and *Gsdmd*$^{-/-}$ mice in a healthy state.
E) Percentage of mature neutrophils among CD45+ CD11b+ Ly6G+ neutrophils in each organ (n=3-5 per group).
Data represent means ± SD and analyzed using unpaired Student's t-test.

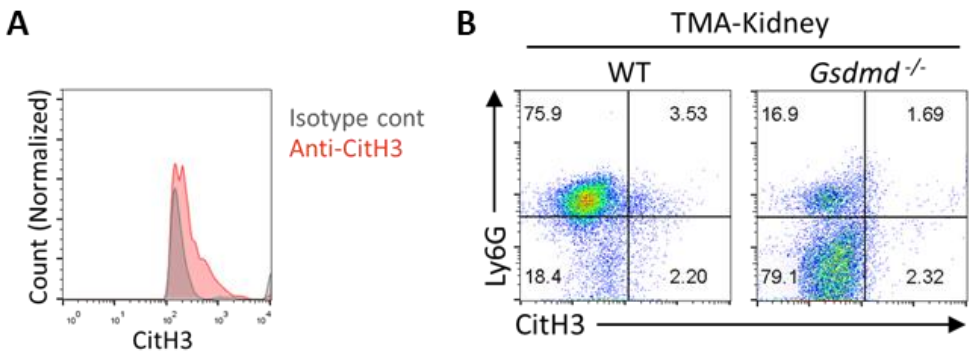

Supplementary figure S6. Identification of NETs in kidneys of WT and *Gsdmd*$^{-/-}$ mice with focal TMA

A) Flow cytometric histogram of isotype control and anti-citrullinated histone 3 (CitH3) antibody-stained kidney samples from wild-type (WT) mice with focal thrombotic microangiopathy (TMA).

B) Representative images of the gating strategy for identifying NETing neutrophils (CD45+ CD11b+ Ly6G+ CitH3+) in kidney from WT and *Gsdmd*$^{-/-}$ mice with focal TMA.

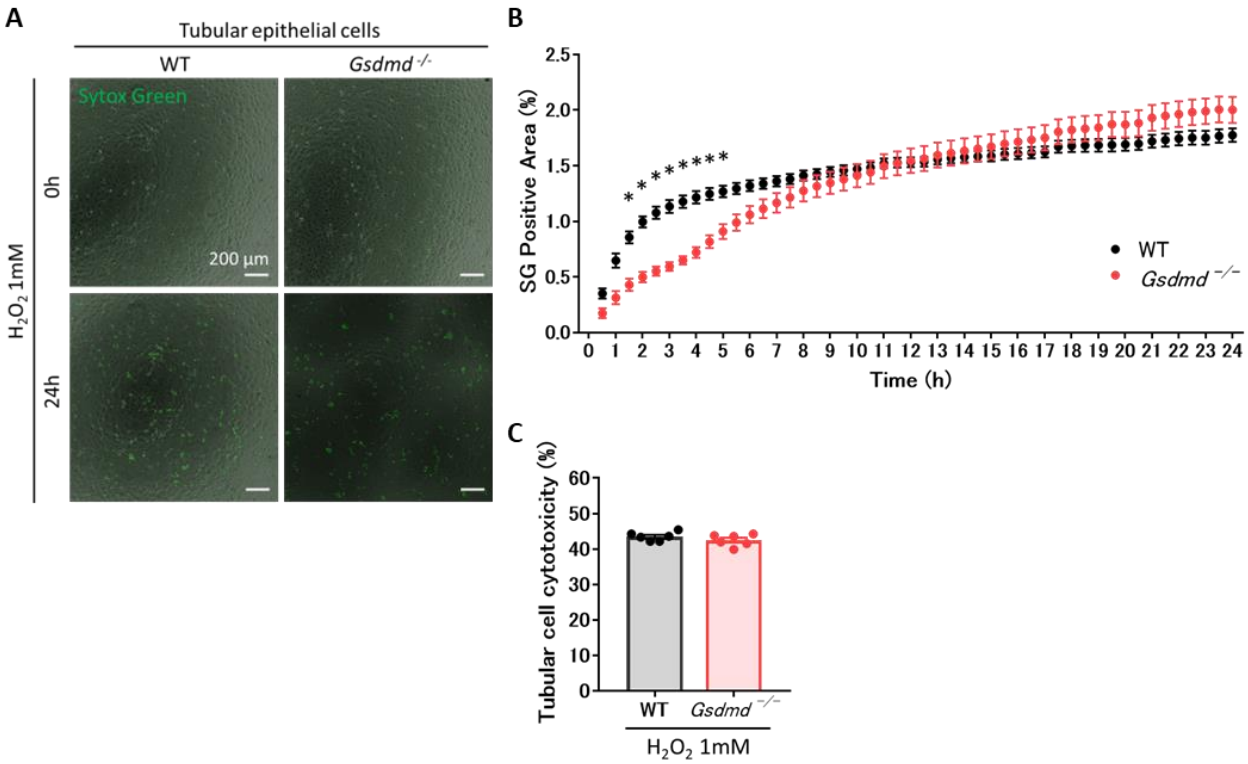

Supplementary figure S7. GSDMD does not contribute to hypoxia-induced tubular cell death

Primary renal tubular cells were isolated from 3- to 4-week-old wild-type (WT) and gasdermin D knockout (*Gsdmd*$^{-/-}$) mice. The cultured cells were seeded at a density of 1×10^5 cells/mL in a 96-well plate. Following an overnight incubation, the cells were exposed to 1 mM H_2O_2 to mimic hypoxia-induced cell death.

A) Representative time-lapse images of the cells stained with SYTOX Green (SG) at 0 hour and 24 hours following the stimulation.

B) SG-positive area in each time point (every 30 minutes for 24 hours).

C) Cytotoxicity analyzed by lactate dehydrogenase assay in the cell-free supernatant collected after 24 hours. Data are representative of two independent experiments.

Scale bars: (A) 200 µm. The data represent means ± SEM. *p < 0.05 using unpaired Student's t-test.

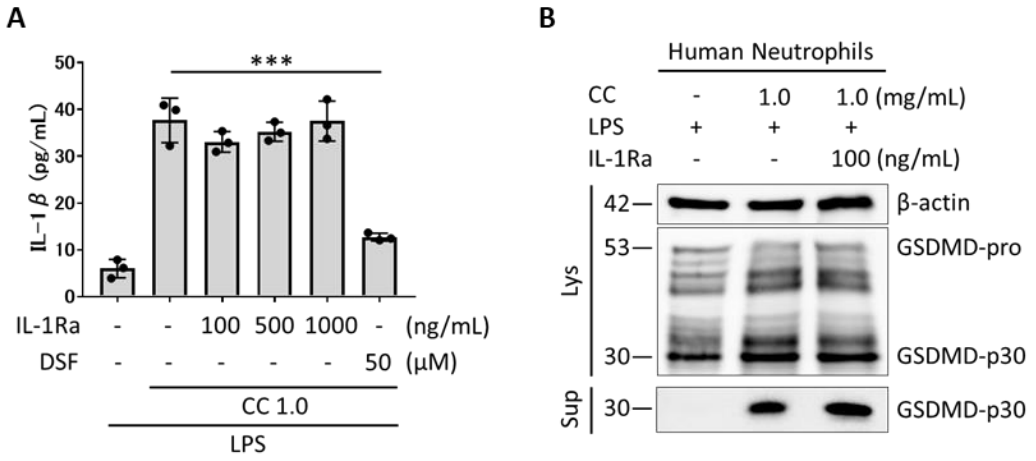

Supplementary figure S8. IL-1β pathway does not impact on GSDMD cleavage and IL-1β release from CC-stimulated neutrophils

Human neutrophils were primed with lipopolysaccharide (LPS) for 2 hours. After pretreatment with disulfiram (DSF) or anakinra, an IL-1 receptor antagonist (IL-1Ra), neutrophils were stimulated with cholesterol crystal (CC, 1 mg/mL) for 3 hours under shaking conditions.

A) Cell-free supernatants were collected for IL-1β ELISA.

B) Cell-free supernatants and cell lysates from 3 wells were combined for each condition and collected for immunoblot analysis of gasdermin D (GSDMD). β-actin was used as a loading control.

The data represent means ± SEM. ***p < 0.001 using one-way ANOVA with Dunnett's multiple comparisons test.

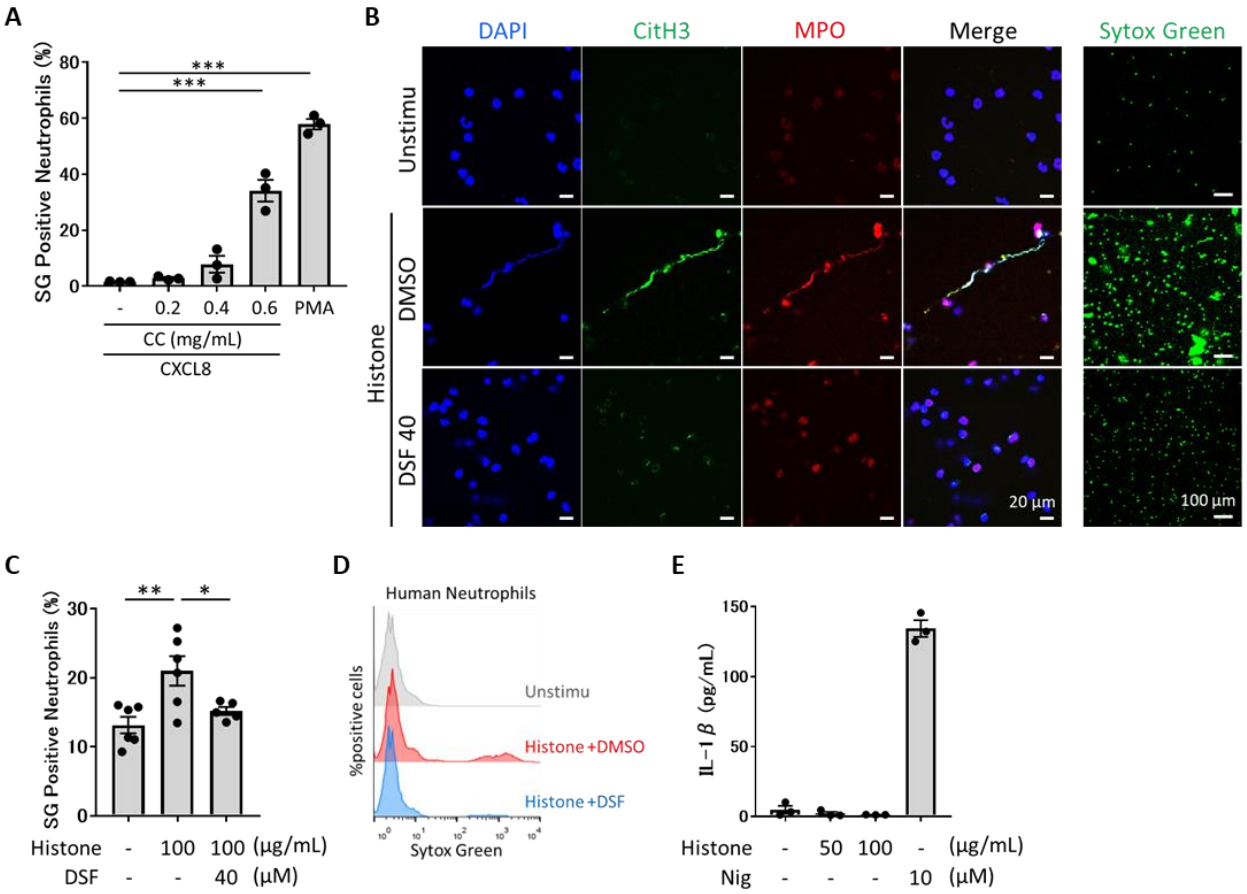

Supplementary figure S9. Disulfiram inhibits histone-induced NETosis in human neutrophils in vitro

A) Human neutrophils were primed with CXCL8, followed by stimulation with cholesterol crystal (CC) or phorbol 12-myristate 13-acetate (PMA, 20 nM) for 3 hours under shaking conditions. The cells were stained with SYTOX Green (SG) and analyzed using flow cytometry.

B) Human neutrophils were primed with CXCL8. After pretreatment with disulfiram (DSF) or dimethyl sulfoxide (DMSO), the cells were stimulated with histone (100 µg/mL). Neutrophil extracellular traps (NETs) were visualized by immunofluorescent images, stained with citrullinated histone 3 (CitH3, green), myeloperoxidase (MPO, red), and 4',6-diamidino-2-phenylindole (DAPI, blue), and by live cell images stained with SG (green).

C) Cells were stained with SG for flow cytometric analysis.

D) Representative histogram for SG positive neutrophils.

E) Cell-free supernatants were collected for interleukin (IL)-1β ELISA. Supernatants from cells after lipopolysaccharide priming and nigericin (10 µM) stimulation for 3 hours were used as a positive control. Scale bars: (B) 20 µm (immunofluorescent images) and 100 µm (live images). The data represent means ± SEM. *p < 0.05, **p < 0.01, and ***p < 0.001 using one-way ANOVA with Dunnett's multiple comparisons test.

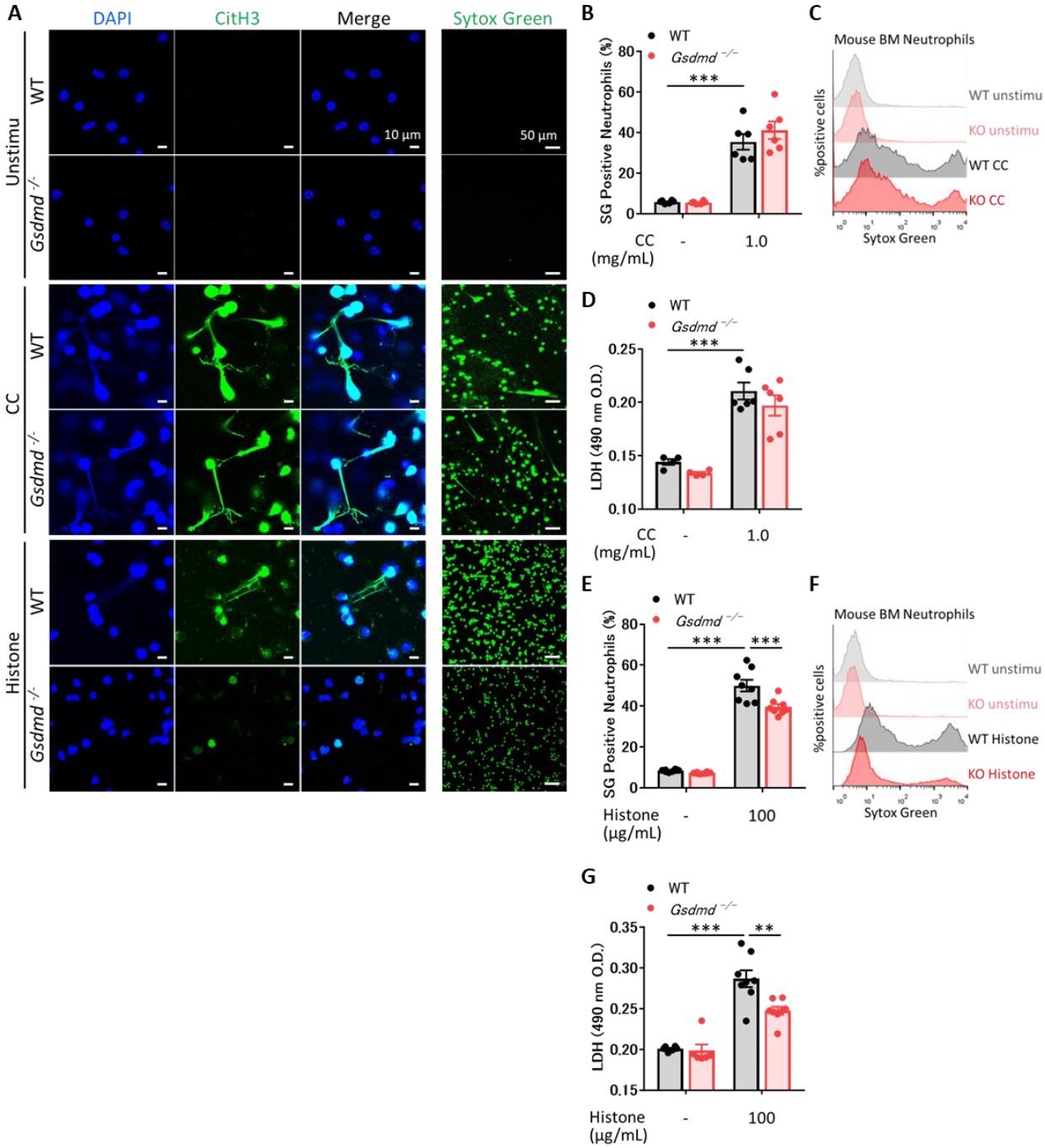

526

527 **Supplementary figure S10. *Gsdmd*$^{-/-}$ mouse neutrophils exhibit comparable levels of CC-induced NET**
528 **formation but attenuate NET formation elicited by histones**

529 Bone marrow neutrophils isolated from wild-type (WT) and gasdermin D knockout *(Gsdmd*$^{-/-}$*)* mice were
530 stimulated with cholesterol crystal (CC) or histone.

531 A) Neutrophil extracellular traps (NETs) were visualized by immunofluorescent images, stained with
532 citrullinated histone 3 (CitH3, green) and 4',6-diamidino-2-phenylindole (DAPI, blue), and by live cell
533 images stained with SYTOX Green (SG, green).

534 B) Cells following CC stimulation were stained with SG for flow cytometric analysis.

535 C) Representative histogram for SG positive neutrophils following CC stimulation.

536 D) Cell-free supernatants following CC stimulation were collected for lactate dehydrogenase (LDH) assay.

E) Cells following histone stimulation were stained with SG for flow cytometric analysis.
F) Representative histogram for SG positive neutrophils following histone stimulation.
G) Cell-free supernatants following histone stimulation were collected for LDH assay.
Scale bars: (A) 10 μm (immunofluorescent images) and 50 μm (live images).The data represent means ± SEM. **p < 0.01 and ***p < 0.001 using two-way ANOVA with Bonferroni's multiple comparisons test.

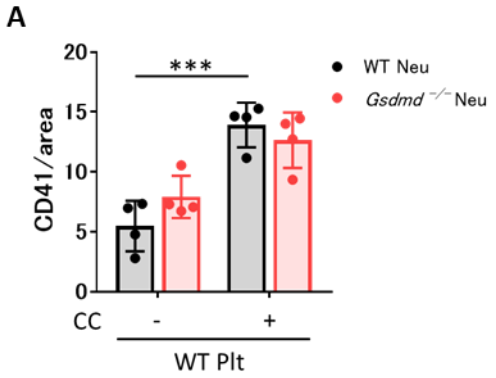

Supplementary figure S11. Cholesterol crystal promotes platelet adhesion on the collagen-coated surface

Heparinized whole blood samples from wild-type (WT) mice were perfused over the collagen-coated surface at 1000 s^{-1} in the presence and absence of cholesterol crystal (CC) using a flow chamber system. In a second-step flow chamber assay, WT and gasdermin D knockout *(Gsdmd*$^{-/-}$) bone marrow neutrophils were perfused over WT platelet-rich thrombi through the chamber at 500 s^{-1}. (A) Quantification of CD41 (platelet marker) signals visualized by immunofluorescence confocal microscopy (n=4 per group).

The data represent means ± SD. ***$p < 0.001$ using two-way ANOVA with Bonferroni's multiple comparisons test.

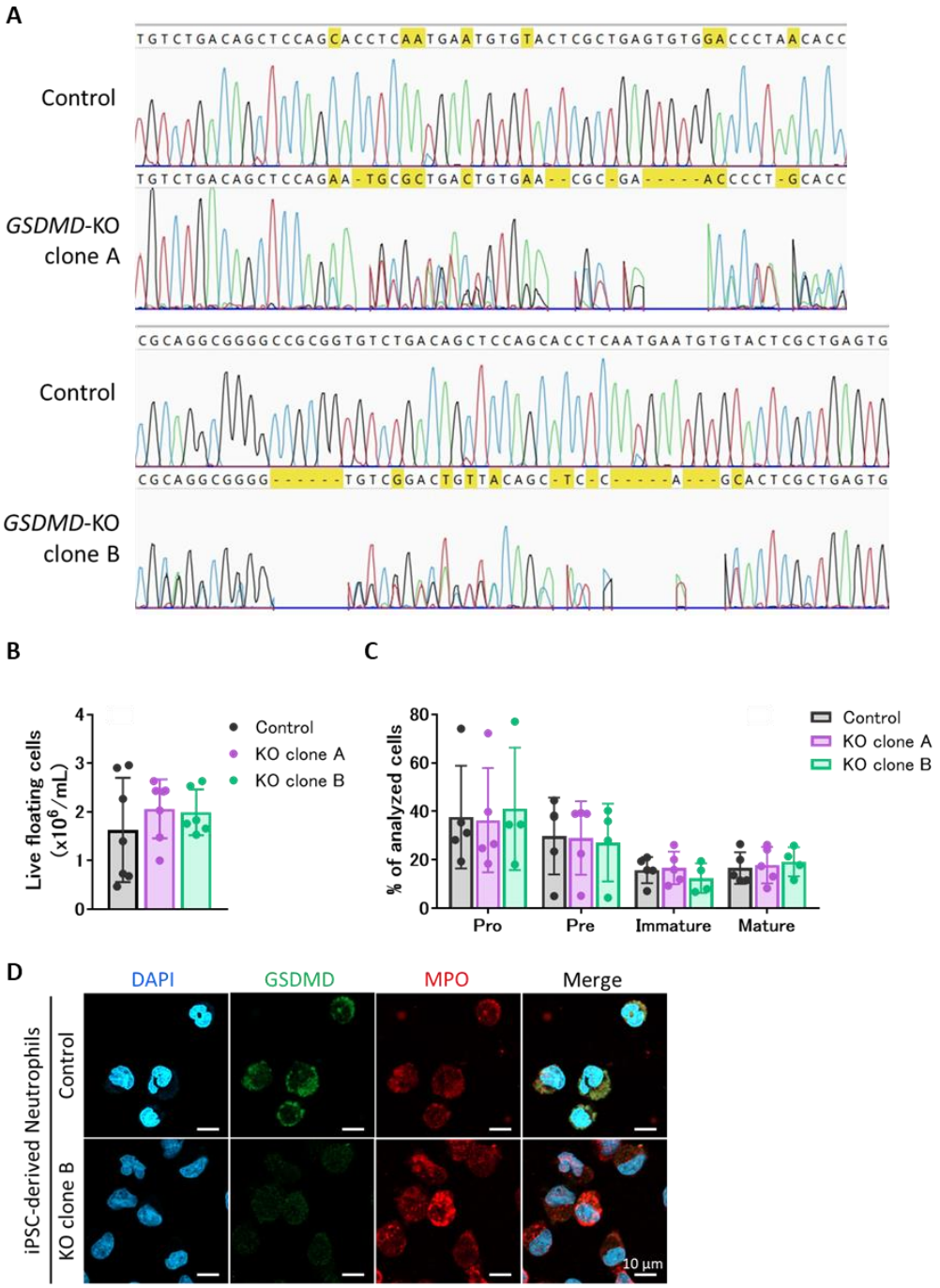

Supplementary figure S12. Characterization of iPSC-derived neutrophils

A) Sanger sequencing on gasdermin D (GSDMD) in *GSDMD*-knockout induced pluripotent stem cell (iPSC)-derived neutrophils, with reference to the control iPSC-derived neutrophils.

B) Number of live floating cells determined at day 28-32 during differentiation of iPSC-derived control and *GSDMD*-knockout neutrophils. The data presents as the mean of six to seven independent experiments.

C) Flow cytometric quantification of pro-neutrophils ($CD49d^{high}$ $CD11b^{-}$), pre-neutrophils ($CD49d^{mid}$ $CD101^{-}$), immature neutrophils ($CD11b^{+}$ $CD101^{+}$), and mature neutrophils ($CD49d^{low}$ $CD11b^{+}$ $CD101^{+}$ $CD16^{+}$) at day 28-32 during differentiation of iPSC-derived control and *GSDMD*-knockout neutrophils. The data presents as the mean of four to five independent experiments.

D) Representative immunofluorescent images of iPSC-derived neutrophils (day 28) stained with GSDMD (green), myeloperoxidase (MPO, red) and 4',6-diamidino-2-phenylindole (DAPI, blue).

Scale bars: (D) 10 μm. Data are analyzed using one-way ANOVA with Dunnett's multiple comparison test (B), or two-way ANOVA with Dunnett's multiple comparison test (C).

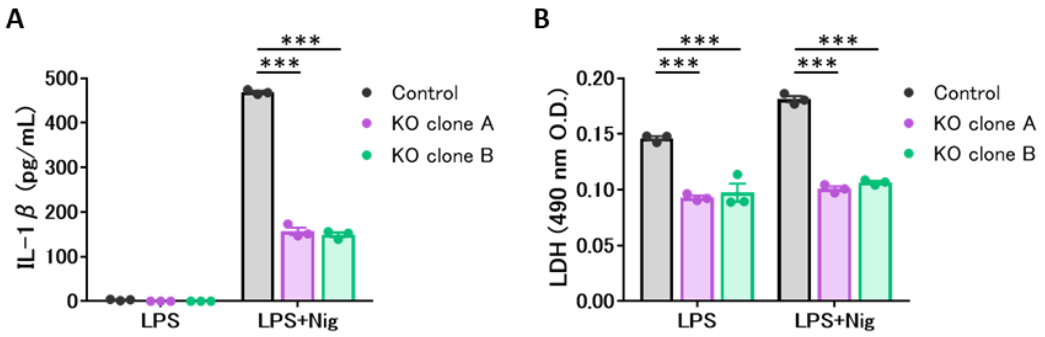

Supplementary figure S13. *GSDMD*-deficient iPSC-derived neutrophils resist nigericin-induced pyroptosis

A)-B) iPSC-derived neutrophils were primed with lipopolysaccharide (LPS) for 4 hours, followed by stimulation with nigericin (10 μM) for 3 hours. Cell-free supernatants were collected for interleukin (IL)-1β ELISA (A) and lactate dehydrogenase (LDH) assay (B).

The data represent means ± SEM. ***$p < 0.001$ using two-way ANOVA with Dunnett's multiple comparisons test. Data are representative of four independent experiments.

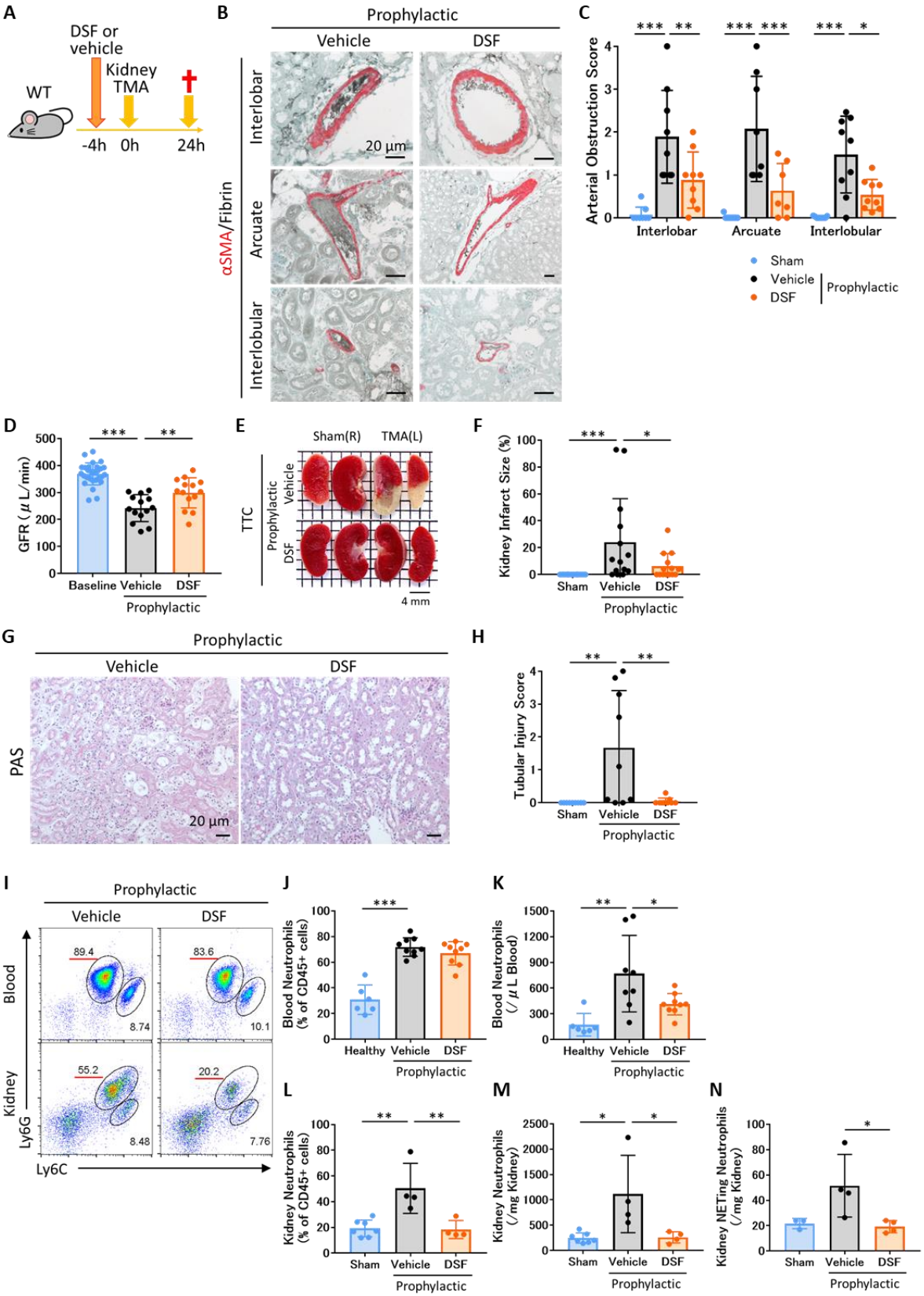

Supplementary figure S14. Prophylactic disulfiram protects mice from TMA, AKI and ischemic infarction

A) Illustration of the experimental design. Wild-type (WT) mice were administered disulfiram (DSF, 50 mg/kg) or vehicle 4 hours prior to crystal injection. The mice were sacrificed and analyzed 24 hours post-

surgery.

B) Representative immunohistochemical images of alpha-smooth muscle actin (αSMA) and fibrin staining of interlobar, arcuate, and interlobular arteries in kidneys with thrombotic microangiopathy (TMA).

C) Quantification of arterial obstruction (n=9 per group).

D) Glomerular filtration rate (GFR) at baseline and 24 hours after focal TMA induction (n=14 per group).

E) Representative images of 2,3,5-Triphenyltetrazolium chloride (TTC) staining on the TMA (left) and sham (contralateral right) kidneys. The red areas indicate living kidney tissue, while the white areas indicate infarcted kidney tissue.

F) Quantification of the kidney infarct size (n=14 per group).

G) Representative images of Periodic acid-Schiff (PAS) staining on TMA kidneys.

H) Quantification of tubular injury (n=9 per group).

I) Representative gating of flow cytometric analysis for the quantification of neutrophils (CD45+ CD11b+ Ly6G+) and monocytes (CD45+ CD11b+ Ly6C+) in blood and kidney following focal TMA induction.

J)-K) Percentage of neutrophils among CD45+ cells (J) and their absolute number (K) in blood from focal TMA mice (n=8-9 per group).

L)-M) Percentage of neutrophils among CD45+ cells (L) and their absolute number (M) in TMA kidneys (n=4 per group).

N) Absolute number of NETing neutrophils (CD45+ CD11b+ Ly6G+ CitH3+) in TMA kidneys (n=4 per group) determined by flow cytometry.

Scale bars: (B) and (G) 20 μm, (E) 4 mm. The data represent means ± SD. *$p < 0.05$, **$p < 0.01$, and ***$p < 0.001$ using two-way ANOVA with Bonferroni's multiple comparisons test (C), or one-way ANOVA with Tukey's post-hoc test (D, F, H, J-N).

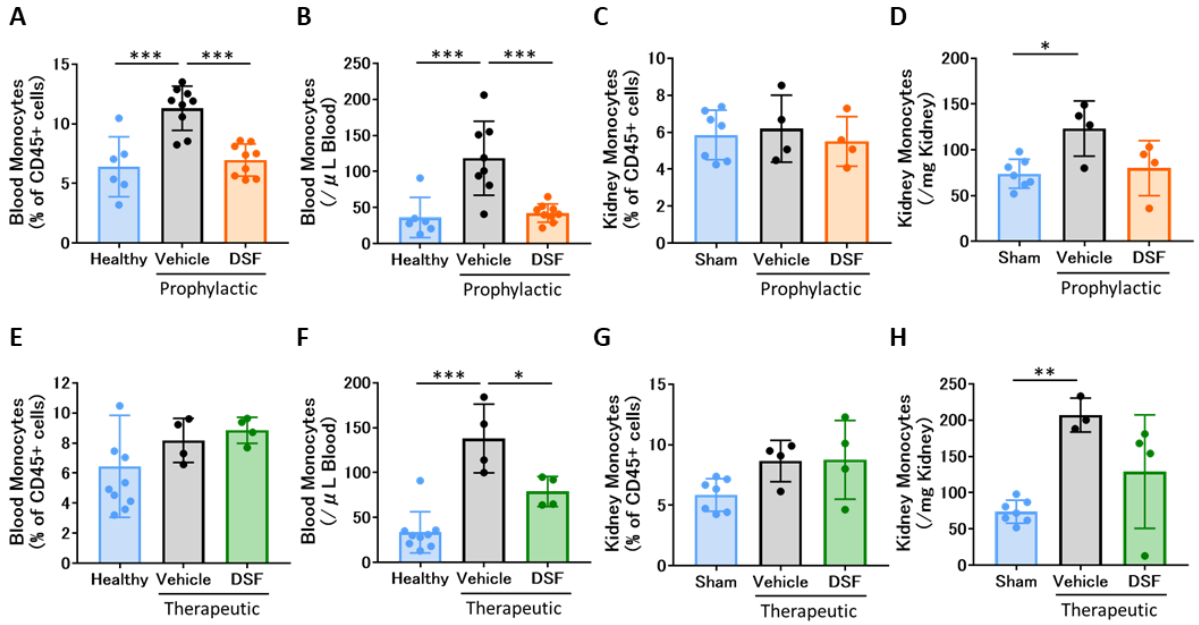

608

609

610 **Supplementary figure S15. The number of monocytes in blood and kidney of TMA mice with**
611 **disulfiram treatment**

612 A)-B) Percentage of monocytes among CD45+ cells (A) and their absolute number (B) in blood from focal
613 thrombotic microangiopathy (TMA) mice with prophylactic disulfiram (DSF) treatment (n=9 per group).
614 C)-D) Percentage of monocytes among CD45+ cells (C) and their absolute number (D) in kidney from focal
615 TMA mice with prophylactic DSF treatment (n=4 per group).
616 E)-F) Percentage of monocytes among CD45+ cells (E) and their absolute number (F) in blood from focal
617 TMA mice with therapeutic DSF treatment (n=4 per group).
618 G)-H) Percentage of monocytes among CD45+ cells (G) and their absolute number (H) in kidney from focal
619 TMA mice with therapeutic DSF treatment (n=3-4 per group).
620 The data represent means ± SD. *$p < 0.05$, **$p < 0.01$, and ***$p < 0.001$ using one-way ANOVA with Tukey's
621 post-hoc test.

622

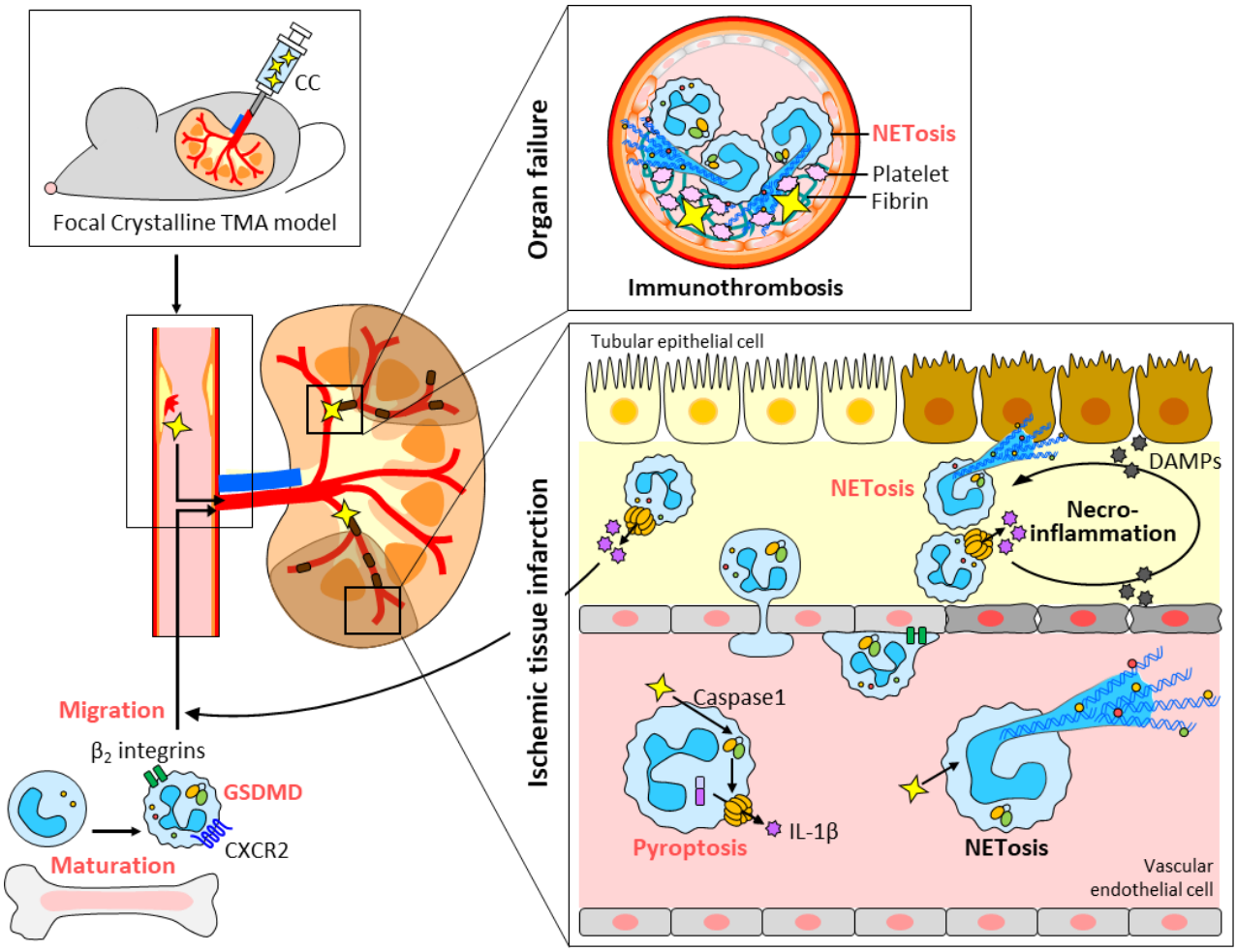

Supplementary figure S16. Graphical abstract

Gasdermin D (*Gsdmd*)-deficiency ameliorated intravascular immunothrombosis and its consequences, ischemic tissue infarction and organ failure, in a murine model of cholesterol crystal (CC)-induced focal thrombotic microangiopathy (TMA). Mechanistically, GSDMD facilitates the activation of β_2 integrins and the maturation of neutrophils, both of which promote their egress and migration from bone marrow to blood and inflamed tissue. The migrated neutrophils collaborate with CC-triggered activated platelets in a GSDMD-dependent manner, forming intravascular neutrophil extracellular traps (NETs). These NETs promote immunothrombosis, leading to arterial occlusion and subsequent organ failure. Furthermore, GSDMD facilitates CC-induced neutrophil pyroptosis and the release of IL-1β, thereby promoting tissue necroinflammation, subsequent NET formation, and further neutrophil recruitments. Pharmacological blockade of GSDMD protected the mice from focal crystalline TMA and its associated consequences. These findings identify GSDMD as a key mediator of focal crystalline TMA and its consequences, tissue necroinflammation and organ failure.

Supplementary References

1. Shi C, Kim T, Steiger S, et al. Crystal Clots as Therapeutic Target in Cholesterol Crystal Embolism. *Circ Res*. 2020.
2. Warnatsch A, Ioannou M, Wang Q, Papayannopoulos V. Inflammation. Neutrophil extracellular traps license macrophages for cytokine production in atherosclerosis. *Science*. 2015;349(6245):316-320.
3. Schreiber A, Shulhevich Y, Geraci S, et al. Transcutaneous measurement of renal function in conscious mice. *Am J Physiol Renal Physiol*. 2012;303(5):F783-788.
4. Friedemann J, Heinrich R, Shulhevich Y, et al. Improved kinetic model for the transcutaneous measurement of glomerular filtration rate in experimental animals. *Kidney Int*. 2016;90(6):1377-1385.
5. Steiger S, Grill JF, Ma Q, et al. Anti-Transforming Growth Factor beta IgG Elicits a Dual Effect on Calcium Oxalate Crystallization and Progressive Nephrocalcinosis-Related Chronic Kidney Disease. *Front Immunol*. 2018;9:619.
6. Liu F, Schafer DP, McCullough LD. TTC, fluoro-Jade B and NeuN staining confirm evolving phases of infarction induced by middle cerebral artery occlusion. *J Neurosci Methods*. 2009;179(1):1-8.
7. Ma Q, Immler R, Pruenster M, et al. Soluble uric acid inhibits β2 integrin-mediated neutrophil recruitment in innate immunity. *Blood*. 2022;139(23):3402-3417.
8. Lech M, Grobmayr R, Ryu M, et al. Macrophage phenotype controls long-term AKI outcomes--kidney regeneration versus atrophy. *J Am Soc Nephrol*. 2014;25(2):292-304.
9. Jiang K, Tu Z, Chen K, et al. Gasdermin D inhibition confers antineutrophil-mediated cardioprotection in acute myocardial infarction. *J Clin Invest*. 2022;132(1).
10. Martinod K, Witsch T, Erpenbeck L, et al. Peptidylarginine deiminase 4 promotes age-related organ fibrosis. *J Exp Med*. 2017;214(2):439-458.
11. Gavillet M, Martinod K, Renella R, et al. Flow cytometric assay for direct quantification of neutrophil extracellular traps in blood samples. *Am J Hematol*. 2015;90(12):1155-1158.
12. Hornung V, Bauernfeind F, Halle A, et al. Silica crystals and aluminum salts activate the NALP3 inflammasome through phagosomal destabilization. *Nat Immunol*. 2008;9(8):847-856.
13. Zhao ZB, Marschner JA, Iwakura T, et al. Tubular Epithelial Cell HMGB1 Promotes AKI-CKD Transition by Sensitizing Cycling Tubular Cells to Oxidative Stress: A Rationale for Targeting HMGB1 during AKI Recovery. *J Am Soc Nephrol*. 2023;34(3):394-411.
14. Yao W, Chen Y, Li Z, et al. Single Cell RNA Sequencing Identifies a Unique Inflammatory Macrophage Subset as a Druggable Target for Alleviating Acute Kidney Injury. *Adv Sci (Weinh)*. 2022;9(12):e2103675.
15. Lun AT, McCarthy DJ, Marioni JC. A step-by-step workflow for low-level analysis of single-cell RNA-seq data with Bioconductor. *F1000Res*. 2016;5:2122.
16. Korsunsky I, Millard N, Fan J, et al. Fast, sensitive and accurate integration of single-cell data with Harmony. *Nat Methods*. 2019;16(12):1289-1296.

17. Satija R, Farrell JA, Gennert D, Schier AF, Regev A. Spatial reconstruction of single-cell gene expression data. *Nat Biotechnol*. 2015;33(5):495-502.
18. Xie X, Shi Q, Wu P, et al. Single-cell transcriptome profiling reveals neutrophil heterogeneity in homeostasis and infection. *Nat Immunol*. 2020;21(9):1119-1133.